Z. Phys. Chem. **225** (2011) 413–419 / **DOI** 10.1524/zpch.2011.0115

Phase Behaviour of $CoCl_2$-$MnCl_2$ Mixed Crystals

By Jav Davaasambuu[1], Friedrich Güthoff[1], Markus Hoelzel[2], Anatoliy Senyshyn[2], Aurel Radulescu[3], and Götz Eckold[1,*]

[1] Institute of Physical Chemistry, University of Göttingen, Germany
[2] Department of Materials and Earth Sciences, TU Darmstadt, Germany
[3] Jülich Centre for Neutron Science, Forschungszentrum Jülich GmbH, Germany

(Received February 9, 2011; accepted in revised form March 2, 2011)

Mixed Crystal / Demixing / Phase Diagram / Neutron Diffraction / Neutron Small Angle Scattering

Thermal properties of $CoCl_2$, $MnCl_2$ and their mixed crystals are investigated by means of temperature dependent neutron powder diffraction and time-resolved small angle neutron scattering. The coefficients of thermal expansion of these crystals have been determined as a function of temperature. The temperature-induced structural variations can be explained by distortions of $CoCl_6/MnCl_6$ octahedra and changes in Co/Mn–Cl bond lengths. $CoCl_2$ and $MnCl_2$ form homogeneous solid solutions in the entire temperature range between the solidus and 50 K. There is no indication of any miscibility gap as predicted from thermodynamic calculations.

1. Introduction

Demixing reactions in solids can be used for the preparation of self-organised nanoscaled structures if phase separation is dominated by spinodal decomposition. Controlling its kinetics by suitable ageing conditions allows one to predict the characteristic length scales [1]. A necessary condition for this type of demixing is a pronounced miscibility gap along with a suitable lattice parameter mismatch of the constituents. In silver-alkali halides, the phase separation process has been studied in some detail in the past [2–4]. Systems with magnetic ions like cobalt or manganese, however, are not yet studied even if these could principally be used to generate magnetic nano-structures. Interestingly, even the phase diagrams are unknown for most of the binary halide systems. The system $CoCl_2$-$MnCl_2$ could principally provide a suitable magnetic model system since a broad miscibility gap with an upper critical temperature of about 109 °C has been predicted on the thermodynamic calculations [5]. The crystal structures of the pure compounds $CoCl_2$ and $MnCl_2$ have been determined at ambient conditions by Ferrari *et al.* [6] and by Tornedo *et al.* [7], respectively, both exhibiting the trigonal space group R-3m with lattice parameters $a = 3.553$ Å, $c = 17.39$ Å

* Corresponding author. E-mail: geckold@gwdg.de

($a = 3.711$ Å, $c = 17.59$ Å for $MnCl_2$). The crystal lattice consists of layers perpendicular to the [001] direction built from slightly distorted edge sharing $CoCl_6$ ($MnCl_6$) octahedra.

To the best of our knowledge, there are no experimental data available for the mixed system and for other temperatures. Therefore, we have studied the phase behaviour of the system $CoCl_2$-$MnCl_2$ by neutron diffraction as well as neutron small angle scattering in the temperature range between 50 and 500 K. The large contrast of neutron scattering lengths between cobalt (2.49×10^{-15} m) and manganese (-3.73×10^{-15} m) guarantees that any phase separation should become visible. These investigations were complemented by atomic force microscopy.

2. Experimental

$CoCl_2$ and $MnCl_2$ powders were purchased from Merck KGaA (Darmstadt, Germany) and ACROS Organics (Geel, Belgium). Polycrystalline samples of the solid solution with composition $Co_{0.5}Mn_{0.5}Cl_2$ were synthesized from the pure $CoCl_2$ and $MnCl_2$ compounds within sealed quartz ampoules at 750 °C. Due to the hygroscopic nature of the pure constituents, all further sample preparations were performed under argon-gas within a glove box. For the AFM investigations, single crystals were grown in quartz ampoules in a vertical Bridgman furnace. The crystals were cleaved along the [001] planes.

Temperature dependent powder diffraction experiments were carried out at the high-resolution powder diffractometer SPODI at the neutron source FRM-II in Garching [8]. A vertically focussing Ge(551)-monochromator was used to provide neutrons with the wavelength of 1.548 Å at a take-off angle of 155°. The range of scattering angles up to 160° was covered by an array of 80 position sensitive ^{3}He-detectors.

Time-resolved small angle neutron scattering experiments were performed at the KWS-2 instrument at FRM-II [9]. The wavelength of the neutron beam was 4.5 Å. The detector was a 60×60 cm^2 Anger-type scintillation detector with the spatial resolution of 5.25×5.25 mm^2. The sample-detector distance was chosen to cover a Q-range between 0.008 Å^{-1} to 0.3 Å^{-1} thus allowing to detect precipitates or concentration fluctuations with characteristic length scales between 1 nm and 100 nm.

A high resolution non-contact AFM (Omicron UHV-STM/AFM) was used to the study the phase imaging of the cleaved surfaces of mixed crystals. The experiments were performed at room temperature and at a pressure of 10^{-10} mbar.

3. Results and discussion

3.1 Diffraction

Neutron powder diffraction data were collected from 50 K to 475 K for pure compounds $CoCl_2$ and $MnCl_2$ as well as for the solid solution $Co_{0.5}Mn_{0.5}Cl_2$. A typical powder pattern is shown in Fig. 1. All diffraction data can be fitted to one single trigonal phase according to the structural model of [6] and [7]. Even in the case of the mixed crystal, no splitting of Bragg peaks, or other signatures of phase separation could be observed within the entire temperature range down to 50 K. Diffraction data thus indicate that

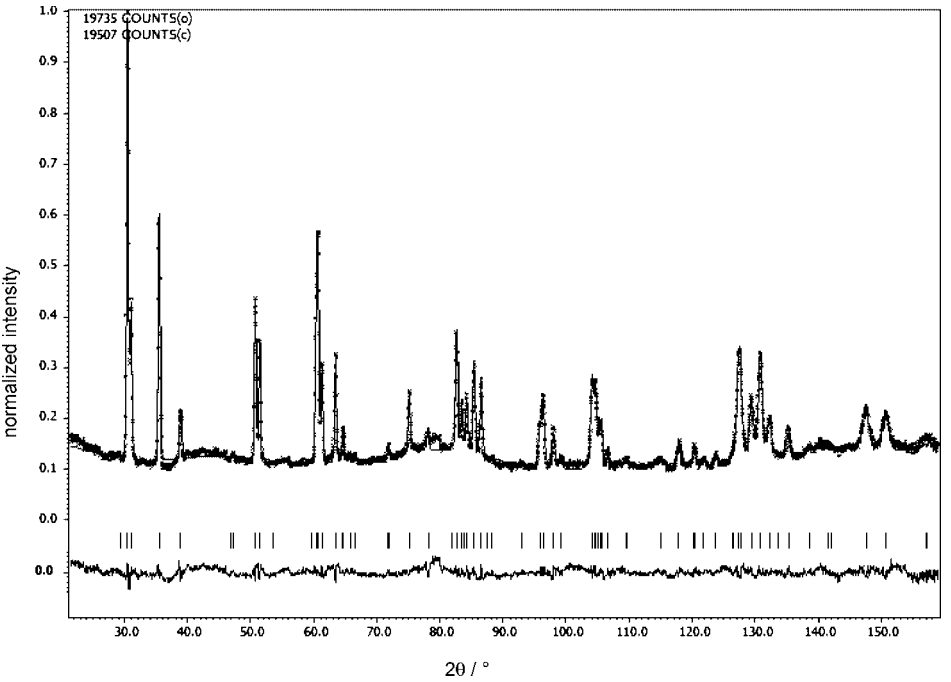

Fig. 1. Powder diffraction pattern of the solid solution $Co_{0.5}Mn_{0.5}Cl_2$ at room temperature.

$CoCl_2$ and $MnCl_2$ are miscible in all proportions and form homogeneous solid solutions even at very low temperatures. Hence, there is a clear discrepancy between the present experimental findings and the theoretical prediction of Robelin *et al.* [5]. The choice of the overall equimolar concentration guarantees that any demixing product would be visible with reasonable intensity given by the lever rule of thermodynamics, unless the miscibility gap were extremely off-symmetrical and did not extend over the 50% limit even at the lowest temperatures. This seems, however, highly improbably since in this case, the solubility of Mn in $CoCl_2$ must be dramatically different from the solubility of Co in $MnCl_2$. In quasibinary mixtures of ionic compounds, such a behaviour has never been observed.

The lattice parameters were determined by Rietveld refinement using FullProf and Jana2006 programs [10,11]. At room temperature, we obtained $a = (3.712 \pm 0.001)$ Å, $c = (17.586 \pm 0.004)$ Å for $MnCl_2$, $a = (3.540 \pm 0.001)$ Å, $c = (17.411 \pm 0.005)$ Å for $CoCl_2$ and $a = (3.629 \pm 0.001)$ Å, $c = (17.501 \pm 0.001)$ Å for $Co_{0.5}Mn_{0.5}Cl_2$. The values for the constituents are in good agreement with previous X-ray measurements [6,7,12,13]. Due to the increased covalency in the Co−Cl bond as compared with Mn−Cl bond, both, a and c, are smaller for $CoCl_2$ as compared to $MnCl_2$. The lattice parameters for the mixed crystal correspond, within the experimental error, to the arithmetic average of both, thus supporting the validity of Végard's rule in this system.

The temperature variation of lattice parameters a and b and the unit cell volume V are shown in Fig. 2 for the three compounds. Note, that the error bars are always smaller

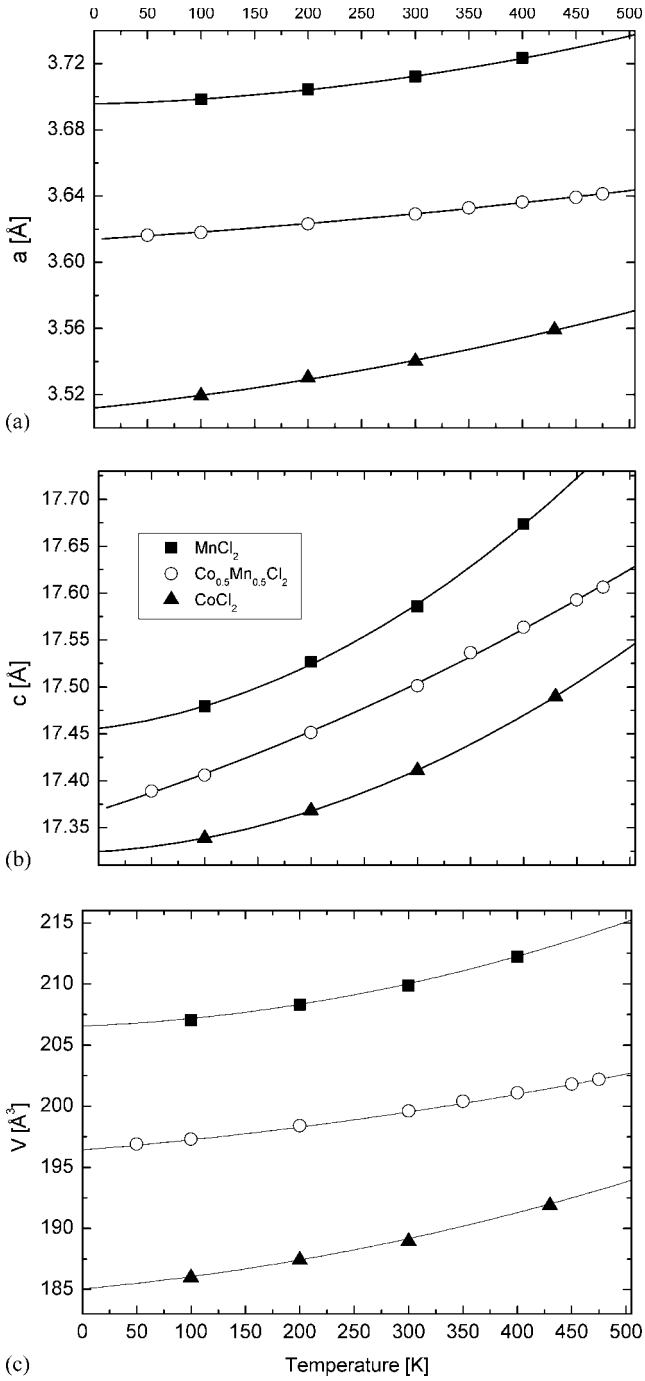

Fig. 2. Temperature variation of lattice parameters *a* (a), *c* (b) and unit cell volume (c) for $MnCl_2$ (■), $CoCl_2$ (▲) and their solid solution (○).

Table 1. Values of the constants in Eqs. (1) and (2) describing the thermal expansion along *a* and *c*.

	a_0 (Å)	a_1 (10^{-6} K^{-1})	a_2 (10^{-8} K^{-2})	c_0 (Å)	c_1 (10^{-6} K^{-1})	c_2 (10^{-7} K^{-2})
$MnCl_2$	3.696 ± 0.001	4.5 ± 3	7.1 ± 1.2	17.46 ± 0.01	8 ± 5	11.5 ± 2.1
$Co_{0.5}Mn_{0.5}Cl_2$	3.614 ± 0.001	8.7 ± 0.9	3.3 ± 0.4	17.365 ± 0.007	20 ± 3	3.5 ± 1.2
$CoCl_2$	3.5126 ± 0.003	20 ± 8	5.6 ± 2.8	17.325 ± 0.002	4.1 ± 0.9	8.4 ± 0.3

than the size of the symbols used to represent the data points. It can be seen that the lattice parameters, as well as the volume of all crystals increase non-linearly with temperature. The data can well be represented by a polynomial of order 2, as conveniently represented by:

$$\begin{aligned} a &= a_0 \left(1 + a_1 T + \frac{1}{2} a_2 T^2\right) \\ c &= c_0 \left(1 + c_1 T + \frac{1}{2} c_2 T^2\right) \\ V &= \frac{\sqrt{3}}{2} a^2 c \,. \end{aligned} \tag{1}$$

The coefficients as obtained by least squares fits are listed in Table 1. It is worthwhile to note, that the non-linearity is significantly reduced in the mixed crystal. Consequently, deviations from Végards rule become visible at low temperatures.

In the mixed crystal, the bond length between transition metal and halide ions increases by about 0.01 Å on heating from 50 K to 400 K. At the same time, the distortion of the $CoCl_6$ ($MnCl_6$) octahedra varies from 4.7% to 5.0%[1] providing additional evidence for the anharmonicity of the layered compound.

In first approximation, the coefficients of thermal expansion exhibit a linear temperature dependence according to:

$$\begin{aligned} \beta_a &= \frac{1}{a}\frac{\partial a}{\partial T} = a_1 + \left(a_2 - a_1^2\right) T \approx a_1 + a_2 T \\ \beta_c &= \frac{1}{c}\frac{\partial c}{\partial T} = c_1 + \left(c_2 - c_1^2\right) T \approx c_1 + c_2 T \\ \alpha &= \frac{1}{V}\frac{\partial V}{\partial T} = 2\beta_a + \beta_c \approx 2a_1 + c_1 + (2a_2 + c_2)\, T \,. \end{aligned} \tag{2}$$

As already seen in Fig. 2, the mixed crystal exhibits a considerably smaller temperature dependence of these coefficients as compared to the pure constituents. Consequently the temperature independent parts (a_1, c_1 and V_1) are found to be much larger for $Co_{0.5}Mn_{0.5}Cl_2$.

3.2 Small angle scattering

It is known from investigations of silver-halides systems [2–4] that demixing processes might occur within the rigid frame of the halide-sublattice. In these cases

[1] The distortion is characterised by the relative differences of the octahedra edges.

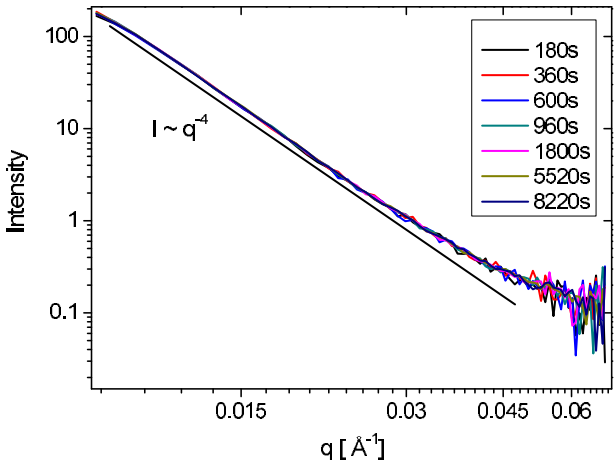

Fig. 3. Time evolution of small angle neutron scattering of the $Co_{0.5}Mn_{0.5}Cl_2$ mixed crystal. For comparison, the Porod-law is represented by the straight line in this double-logarithmic plot.

spinodal decomposition was clearly observed by small angle scattering and by inelastic scattering from phonons while the structural Bragg reflections do not show the characteristic splitting of the equilibrium product phases. It was concluded that spinodal decomposition takes place at almost constant lattice parameter leading to internal coherency strains. Only on a much longer time-scale (of the order of months in the system AgCl-NaCl), mechanical relaxation of the lattice and the corresponding reduction of these strains lead to the final equilibrium state. In those cases, results from diffraction alone are not suitable for the determination of phase diagrams. In order to check whether such behaviour might also be present in the $CoCl_2$-$MnCl_2$ system we have performed small angle scattering experiments in mixed crystals. After quenching a mixed crystals from 250 °C to room temperature, we performed a sequence of the small angle scans over a time scale of several hours. The results are shown in Fig. 3. The scattered intensity decreases monotonically with wave vector transfer q and does not change with time at all. The intensity profile can well be described by the q^{-4}-Porod's law. In particular, there is no evidence for any characteristic feature of spinodal decomposition like a correlation peak that would correspond to concentration fluctuations. If the Porod-behaviour were due to the existence of separate $CoCl_2$ and $MnCl_2$ grains, the quantitative interpretation would lead to grain sizes of the order 5 μm – large enough to produce individual and clearly distinguishable diffraction patterns. Hence, the small angle intensity must be attributed to the grain structure of the homogeneous $Co_{0.5}Mn_{0.5}Cl_2$-phase. Consequently, phase separation can definitely be excluded and the existence of a miscibility gap has to be questioned.

This finding is consistent with complementary investigations using atomic force microscopy of cleaved planes of single crystals. Even on the length scales of nanometers no indications for structural changes due to demixing reactions and the formation of precipitates could be observed.

4. Conclusion

Neutron powder diffraction as well as neutron small angle scattering show that $CoCl_2$ and $MnCl_2$ form a homogeneous solid solution between 50 K and the liquid phase. These is no experimental evidence for the pronounced miscibility gap as predicted by Robelin *et al.* [5]. Hence, it must be concluded that the simple cationic substitutional model (Bragg–Williams) applied by these authors is not adequate to describe the interactions within this system. The temperature variation of the lattice parameters indeed shows the influence of strong anharmonicity leading to a significant variation of the coefficients of thermal expansion. Interestingly, this effect is considerably reduced in mixed crystals that, on the other hand, show a larger thermal expansion at low temperatures as compared to the pure constituents.

Acknowledgement

This work was supported by the DFG under grant EC 153/3-1.

References

1. A. Ringe, P. Elter, H. Gibhardt, and G. Eckold, Solid State Ionics **177** (2006) 2473–2479.
2. P. Elter, G. Eckold, H. Gibhardt, W. Schmidt, and A. Hoser, J. Phys.: Condens. Matter **17** (2005) 6559–6573.
3. G. Eckold, D. Caspary, H. Gibhardt, W. Schmidt, and A. Hoser, J. Phys.: Condens. Matter **16** (2005) 5945–5954.
4. D. Caspary, G. Eckold, F. Güthoff, and W. Pyckhout-Hintzen, J. Phys.: Condens. Matter **13** (2001) 11521.
5. C. Robelin, P. Chartrand, and A. D. Pelton, J. Chem. Thermodynam. **36** (2004) 793–808.
6. A. Ferrari, A. Braibanti, and G. Bigliardi, Acta Cryst. **16** (1963) 846–847.
7. J. D. Tornedo and J. Fayos, Z. Kristallogr. **192** (1990) 147–148.
8. M. Hoelzel, A. Senyshyn, R. Gilles, H. Boysen, and H. Fuess, Neutron News **18** (2007) 23.
9. http://www.jcns.info/jcns_kws2.
10. J. Rodríguez-Carvajal, Phys. B: Condens. Matter **192** (1993) 55–69.
11. V. Petricek and M. Dusek, Z. Kristallogr. **219** (2004) 692–700.
12. G. Bruni and A. Ferrari, Z. Phys. Chem. **130** (1927) 488.
13. H. Grimi and J. A. Santos, Z. Kristallogr. **88** (1934) 136–141.